SAND2022-4476C

Bayesian calibration of interatomic potential models for binary alloys

Arun Hegde
(ahegde@sandia.gov)
Cosmin Safta
Habib Najm

Elan Weiss
Wolfgang Windl

Sandia National Laboratories is a multimission laboratory managed and operated by National Technology & Engineering Solutions of Sandia, LLC, a wholly owned subsidiary of Honeywell International Inc., for the U.S. Department of Energy's National Nuclear Security Administration under contract DE-NA0003525.

Overview

- Interatomic potential models and UQ
- Physical model
- Bayesian calibration
- Running example – Au-Cu binary alloy systems
  - *Posterior predictive* vs. *pushforward posterior* distributions highlight the importance of model error.

Interatomic potentials and UQ

- Interatomic potentials
  - function that takes as input the positions of atoms and returns the energy of the system
  - contains unknown parameters that must be determined empirically
    - comparison with experiment
    - comparison with higher-fidelity theory
      - e.g. density functional theory (DFT)

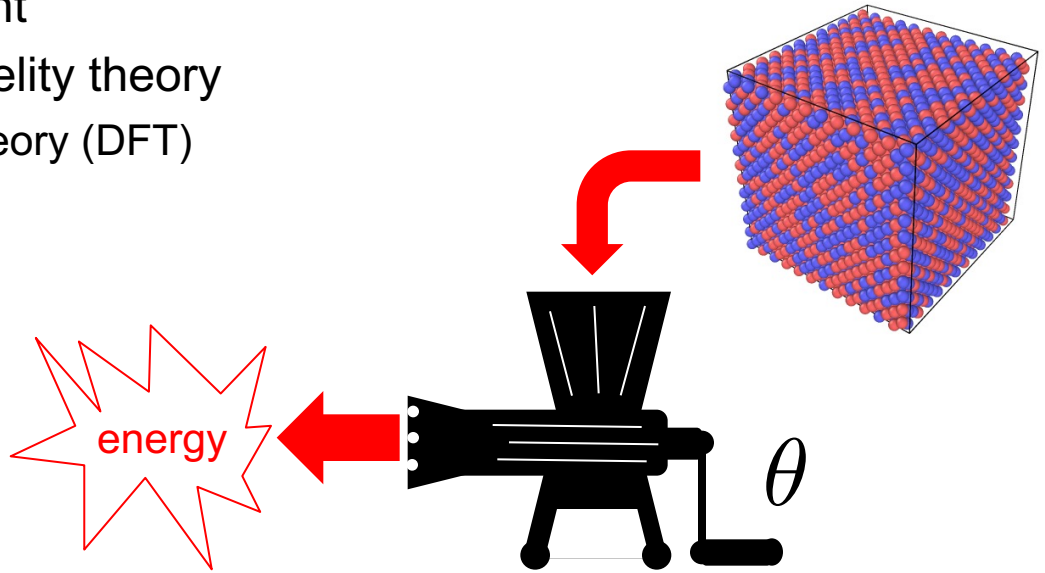

Interatomic potentials and UQ

- Interatomic potentials
  - function that takes as input the positions of atoms and returns the energy of the system
  - contains unknown parameters that must be determined empirically
    - comparison with experiment
    - comparison with higher-fidelity theory
      - e.g. density functional theory (DFT)
- Reliable simulation with interatomic potentials requires quantified uncertainties*
  - for model validation and comparison
  - for prediction
  - for decision-making

*S.L. Frederiksen, K.W. Jacobsen, K.S. Brown, J.P. Sethna, Phys. Rev. Lett. 93, 165501 (2004)

RAMPAGE potentials for binary alloy design

Rapid **A**lloy **M**ethod for **P**roducing **A**ccurate **G**eneral **E**mpirical potentials*

Embedded Atom Model (Finnis-Sinclair type) for systems with <u>two element types: **A** and **B**</u>

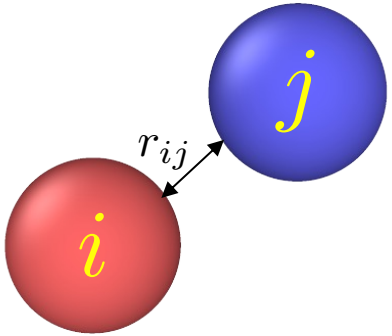

- atom i of type $\alpha \in \{A, B\}$
- atom j of type $\beta \in \{A, B\}$

energy at atom *i*

$$E_i = \frac{1}{2} \sum_{j \neq i} V_{\alpha\beta}(r_{ij}) + F_\alpha \left(\sum_{j \neq i} \rho_{\alpha\beta}(r_{ij}) \right)$$

component functions could each contribute to θ

*L. Ward, A. Agrawal, K.M. Flores, and W. Windl. Rapid production of accurate embedded-atom method potentials for metal alloys. (2012). arXiv:cond-mat.mtrl-sci/1209.0619

RAMPAGE potentials for binary alloy design

Rapid **A**lloy **M**ethod for **P**roducing **A**ccurate **G**eneral **E**mpirical potentials*

Embedded Atom Model (Finnis-Sinclair type) for systems with <u>two element types: **A** and **B**</u>

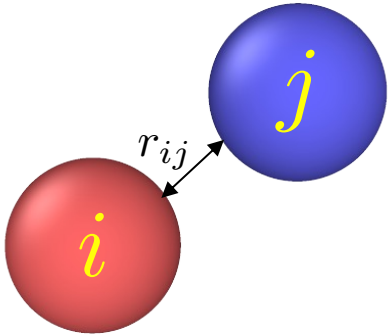

$$F_A \quad \rho_{AA} \quad V_{AA}$$
$$F_B \quad \rho_{BB} \quad V_{BB}$$

extracted from existing literature

already fitted, presumably valid, **no parameters** ✗

$$\rho_{BA} \quad \rho_{AB}$$
$$V_{BA} = V_{AB}$$

modeling and fitting effort, **parameters** ✓

*L. Ward, A. Agrawal, K.M. Flores, and W. Windl. Rapid production of accurate embedded-atom method potentials for metal alloys. (2012). arXiv:cond-mat.mtrl-sci/1209.0619

RAMPAGE potentials for binary alloy design

Rapid **A**lloy **M**ethod for **P**roducing **A**ccurate **G**eneral **E**mpirical potentials*

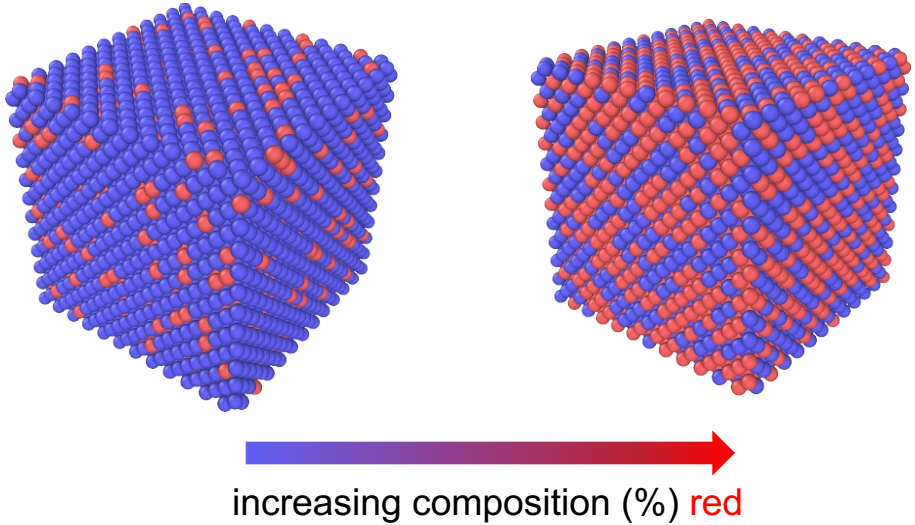

- Generate DFT data for a variety of structures with compositions ranging from 0% A (100%B) to 100% A (0% B).
- Use data to fit the cross-term components of the interatomic potential

*L. Ward, A. Agrawal, K.M. Flores, and W. Windl. Rapid production of accurate embedded-atom method potentials for metal alloys. (2012). arXiv:cond-mat.mtrl-sci/1209.0619

Running example: 5-parameter potential model for Au-Cu

Interatomic potential model

$$V_{AB}(r) = D\left(e^{-2\alpha(r-r_{eq})} - 2e^{-\alpha(r-r_{eq})}\right)$$

Morse pair potential

$$\rho_{BA}(r) = r^6\left(e^{-S_A r} + 2^9 e^{-2S_A r}\right)$$

$$\rho_{AB}(r) = r^6\left(e^{-S_B r} + 2^9 e^{-2S_B r}\right)$$

Voter electron densities

- **5** uncertain parameters: $\theta = [r_{eq}, D, \alpha, S_A, S_B]$
- **102** QOIs total
  - 17 compositions ranging from 3% Au to 97% Au
  - For each composition: **lattice parameter, mixing enthalpy, C11, C12, C44, bulk modulus**
- Higher-fidelity DFT data generated for each QOI
  - used for fitting the uncertain parameters

Workflow for computing QOIs

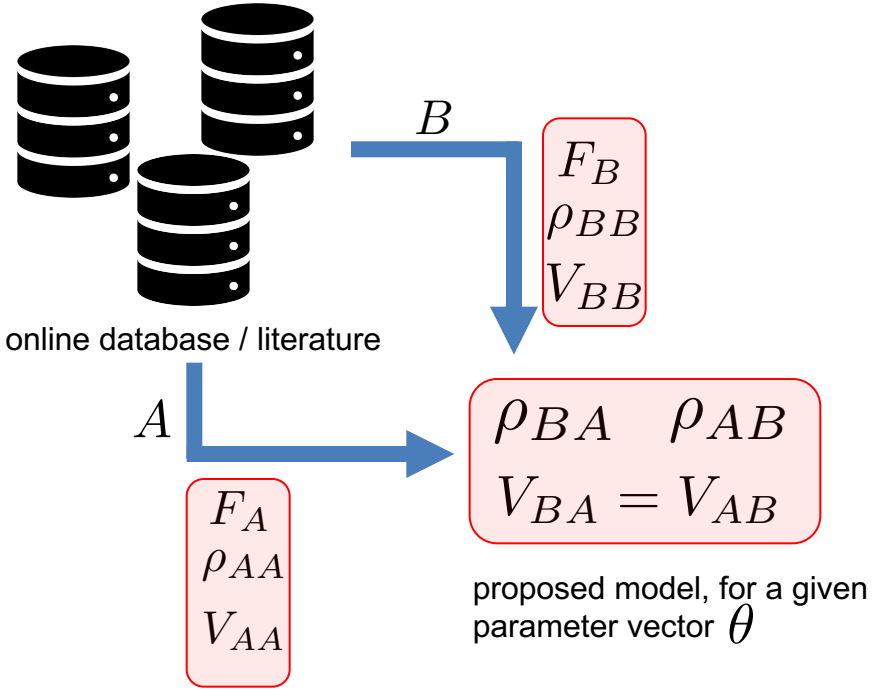

Step 1: download fitted potentials for the pure system, combine with proposed model

Workflow for computing QOIs

online database / literature

B

F_B
ρ_{BB}
V_{BB}

A

F_A
ρ_{AA}
V_{AA}

$\rho_{BA} \quad \rho_{AB}$
$V_{BA} = V_{AB}$

proposed model, for a given parameter vector θ

Step 2: compute quantities of interest using LAMMPS

other inputs:
- structures
- optimization tolerances
- etc.

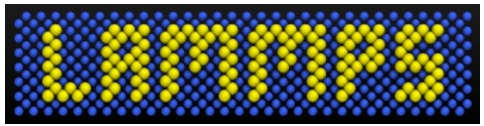

molecular dynamics simulation software*

computed properties & post processing

*image from https://www.lammps.org

Workflow for computing QOIs

online database / literature

B

F_B
ρ_{BB}
V_{BB}

A

F_A
ρ_{AA}
V_{AA}

$\rho_{BA} \quad \rho_{AB}$
$V_{BA} = V_{AB}$

proposed model, for a given parameter vector θ

Step 3: compare to reference DFT data

other inputs:
- structures
- optimization tolerances
- etc.

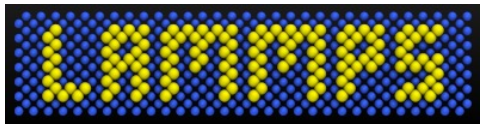

molecular dynamics simulation software*

computed properties & post processing

inference

*image from https://www.lammps.org

Bayesian calibration

finite composition space $x \in \mathcal{X}$

physical properties $i \in \{\text{lat}, \text{mix}, \text{C}_{11}, \text{C}_{12}, \text{C}_{44}, \text{bulk}\}$

notation used to index different **QOIs (102 total)**

$$y_i(x) = f_i(x;\theta) + \epsilon_i(x)$$

DFT data — simulation

simulation

$\theta \in \mathbb{R}^5$ → Interatomic potential model → 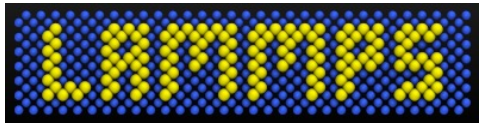

→ $f_i(x;\theta)$

molecular dynamics simulation software*

*image from https://www.lammps.org

Bayesian calibration

finite composition space $x \in \mathcal{X}$

physical properties $i \in \{\text{lat}, \text{mix}, \text{C}_{11}, \text{C}_{12}, \text{C}_{44}, \text{bulk}\}$

notation used to index different **QOIs (102 total)**

$$y_i(x) = f_i(x;\theta) + \epsilon_i(x)$$

DFT data — simulation — model error

$$\epsilon_i(x) \sim \mathcal{N}\left(0, \sigma^2 f_i(x;\theta)^2\right) \qquad i \in \{\text{lat}, \text{C}_{11}, \text{C}_{12}, \text{C}_{44}, \text{bulk}\}$$

$$\epsilon_i(x) \sim \mathcal{N}\left(0, \sigma^2 f_i(x;\theta)^2 + \tau^2\right) \qquad i \in \{\text{mix}\}$$

$$\star \quad \lambda = [\theta, \log\sigma, \log\tau]$$

Bayesian calibration

finite composition space $x \in \mathcal{X}$

physical properties $i \in \{\text{lat}, \text{mix}, \text{C}_{11}, \text{C}_{12}, \text{C}_{44}, \text{bulk}\}$

notation used to index different **QOIs (102 total)**

$$p(\lambda|y) = \frac{p(y|\lambda)p(\lambda)}{p(y)}$$

$\epsilon_i(x) \sim$

$\epsilon_i(x) \sim$

$, \text{C}_{12}, \text{C}_{44}, \text{bulk}\}$

$[\theta, \log\sigma, \log\tau]$

Inference strategy

- Standard strategy
  1. specify a reasonable prior, e.g. uniform over a plausible range
  2. perform MCMC with the full model (i.e. LAMMPS)
  3. analyze posterior samples
- Challenges
  1. not always clear how to specify prior parameter ranges
  2. simulation runtime depends on the input parameter choices
     - single evaluation ~15 minutes – 1hrs+ on a single cpu
  3. regions of the parameter space lead to unphysical results
     - unconverged minimizations, flat QOI response, kinks, etc. (next slide)

Inference strategy

- Standard strategy
  1. specify a reasonable prior, e.g. uniform over a plausible range
  2. perform MCMC with the full model (i.e. LAMMPS)
  3. analyze posterior samples
- Challenges
  1. not always clear how to specify prior parameter ranges
  2. simulation runtime depends on the input parameter choices
     - single evaluation ~15 minutes – 1hrs+ on a single cpu
  3. regions of the parameter space lead to unphysical results
     - unconverged minimizations, flat QOI response, kinks, etc. (next slide)

Illustrations of challenge #2

2D slices of the simulation response

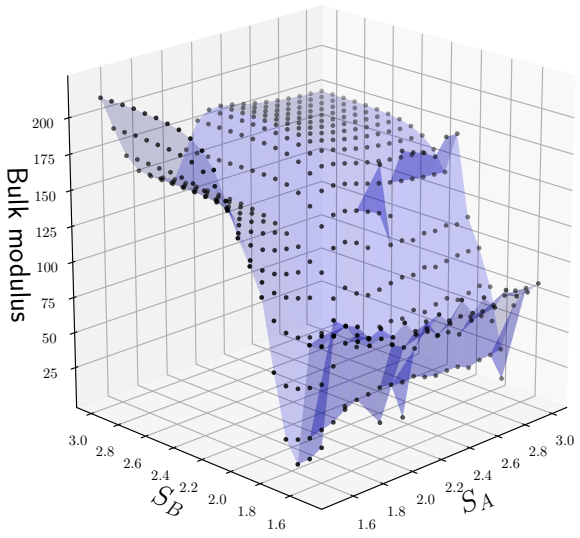

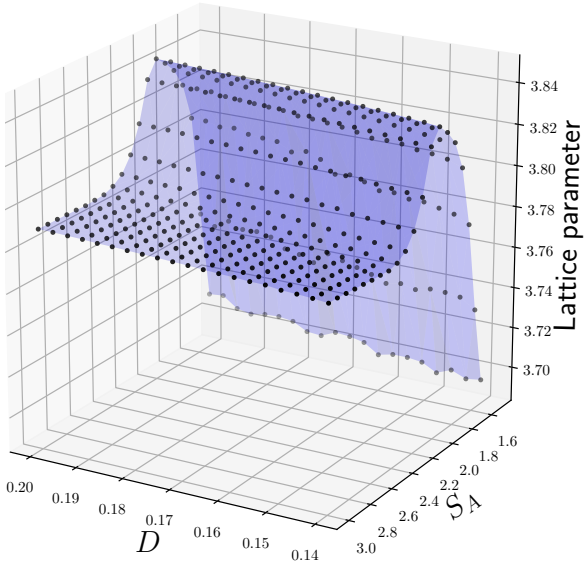

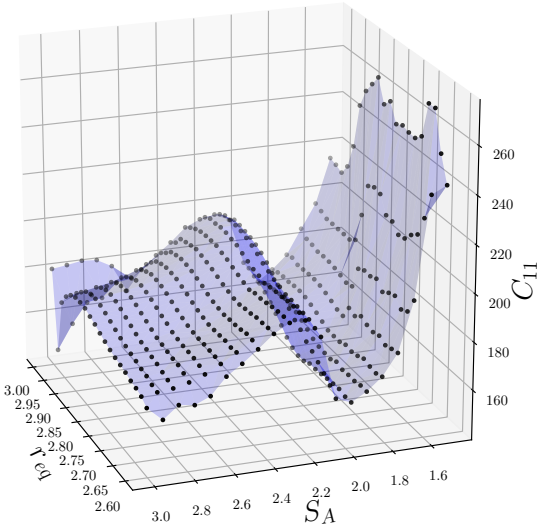

Building globally accurate surrogate models for this parameter-to-QoI mapping is both challenging and inefficient.

Inference strategy

Strategy

1. Find a good initial box in the parameter space.
2. Initialize a set of training/test samples.
3. Fit Gaussian process surrogates.
4. Perform MCMC (with surrogates, uniform prior).
5. Adapt box based on posterior samples.
6. Append posterior samples to training set.
7. Repeat steps **3-6** until:
   - surrogate error on training/test samples is small
   - posterior samples strictly contained

(found through optimization or "expert opinion")

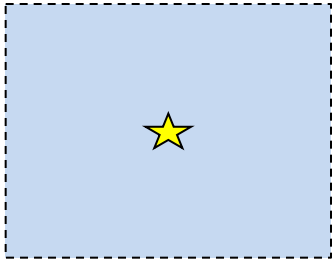

Inference strategy

Strategy

1. Find a good initial box in the parameter space.
2. Initialize a set of training/test samples.
3. Fit Gaussian process surrogates.
4. Perform MCMC (with surrogates, uniform prior).
5. Adapt box based on posterior samples.
6. Append posterior samples to training set.
7. Repeat steps **3-6** until:
   - surrogate error on training/test samples is small
   - posterior samples strictly contained

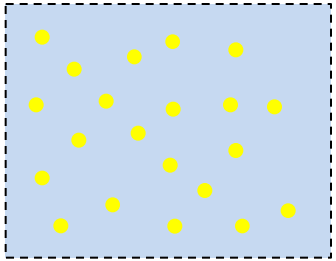

LAMMPS evaluations performed “offline” in a highly parallelized HPC setting

Inference strategy

Strategy

1. Find a good initial box in the parameter space.
2. Initialize a set of training/test samples.
3. Fit Gaussian process surrogates.
4. Perform MCMC (with surrogates, uniform prior).
5. Adapt box based on posterior samples.
6. Append posterior samples to training set.
7. Repeat steps **3-6** until:
   - surrogate error on training/test samples is small
   - posterior samples strictly contained

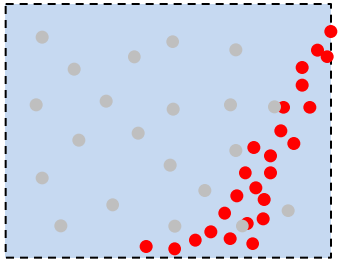

Inference strategy

Strategy

1. Find a good initial box in the parameter space.
2. Initialize a set of training/test samples.
3. Fit Gaussian process surrogates.
4. Perform MCMC (with surrogates, uniform prior).
5. Adapt box based on posterior samples.
6. Append posterior samples to training set.
7. Repeat steps **3-6** until:
   - surrogate error on training/test samples is small
   - posterior samples strictly contained

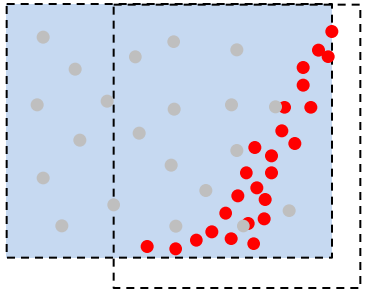

Inference strategy

Strategy

1. Find a good initial box in the parameter space.
2. Initialize a set of training/test samples.
3. Fit Gaussian process surrogates.
4. Perform MCMC (with surrogates, uniform prior).
5. Adapt box based on posterior samples.
6. Append posterior samples to training set.
7. Repeat steps **3-6** until:
   - surrogate error on training/test samples is small
   - posterior samples strictly contained

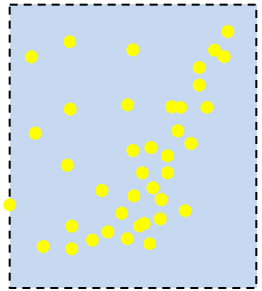

LAMMPS evaluations of new samples performed "offline" in a highly parallelized HPC setting

Inference strategy

Strategy

1. Find a good initial box in the parameter space.
2. Initialize a set of training/test samples.
3. Fit Gaussian process surrogates.
4. Perform MCMC (with surrogates, uniform prior).
5. Adapt box based on posterior samples.
6. Append posterior samples to training set.
7. Repeat steps **3-6** until:
   - surrogate error on training/test samples is small
   - posterior samples strictly contained

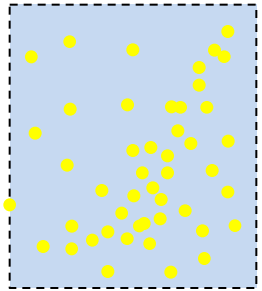

(may also add new samples)

LAMMPS evaluations of new samples performed “offline” in a highly parallelized HPC setting

Return of the running example: Au-Cu system

- Interatomic potential model
  - RAMPAGE potential, single element terms for Au* and Cu*
  - 5-parameter cross-term model
- 102 QoIs in total
  - 17 compositions ranging from 3% Au to 97% Au
  - for each composition: lattice parameter, mixing enthalpy, C11, C12, C44, bulk modulus
- Higher-fidelity DFT data generated for each QoI
  - used for fitting the uncertain parameters
- MCMC algorithm: Adaptive Metropolis

*X. W. Zhou, R. A. Johnson, H. N. G. Wadley, Phys. Rev. B, 69, 144113 (2004)

Results: posterior marginals

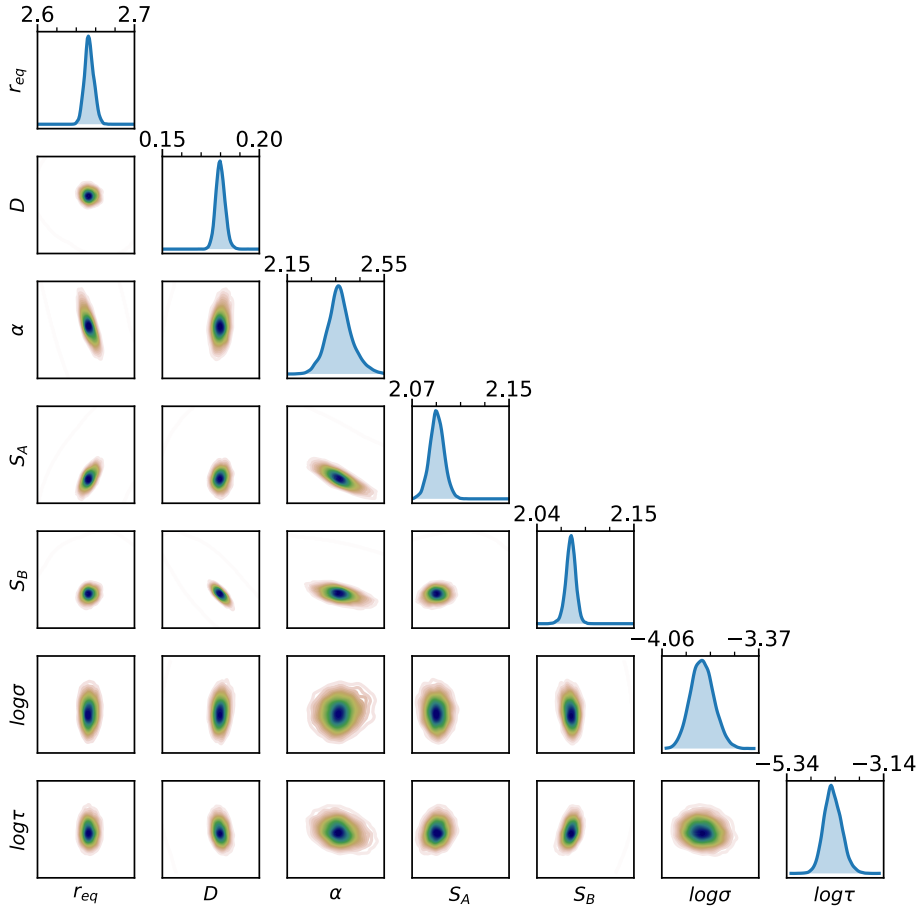

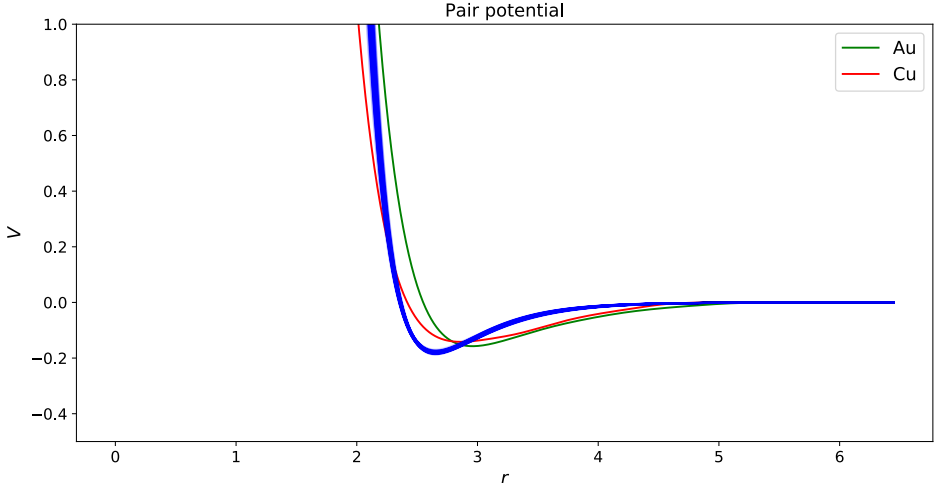

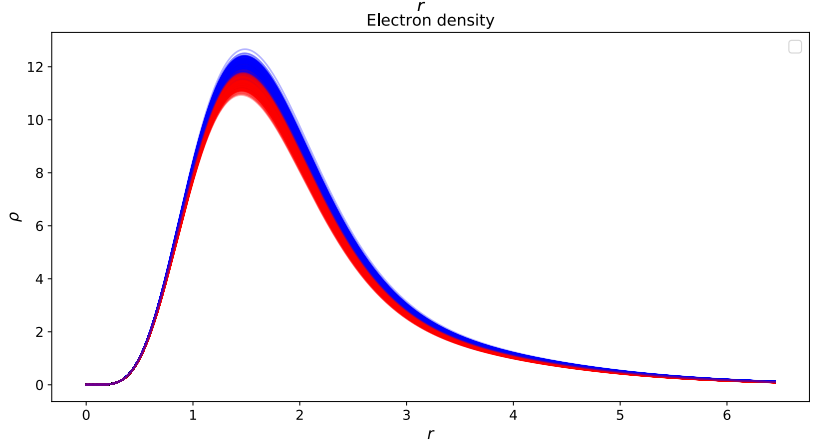

Predictive uncertainty

DFT data: $y_i(x)$ = physical model: $f_i(x;\theta)$ + model error: $\epsilon_i(x)$

Posterior predictive

$p(\lambda|y)$ → physical model + model error → $p_{\text{ppd}}(\tilde{y}|y)$

$\lambda = [\theta, \log\sigma, \log\tau]$

Pushforward posterior*

$p(\theta|y)$ → physical model → $p_{\text{pfp}}(\tilde{y}|y)$

*Sargsyan, K., H. N. Najm, and R. Ghanem. "On the statistical calibration of physical models." *International Journal of Chemical Kinetics* 47.4 (2015): 246-276.

Results: QoI predictions

posterior predictive (left, grey), pushforward posterior (right, blue)

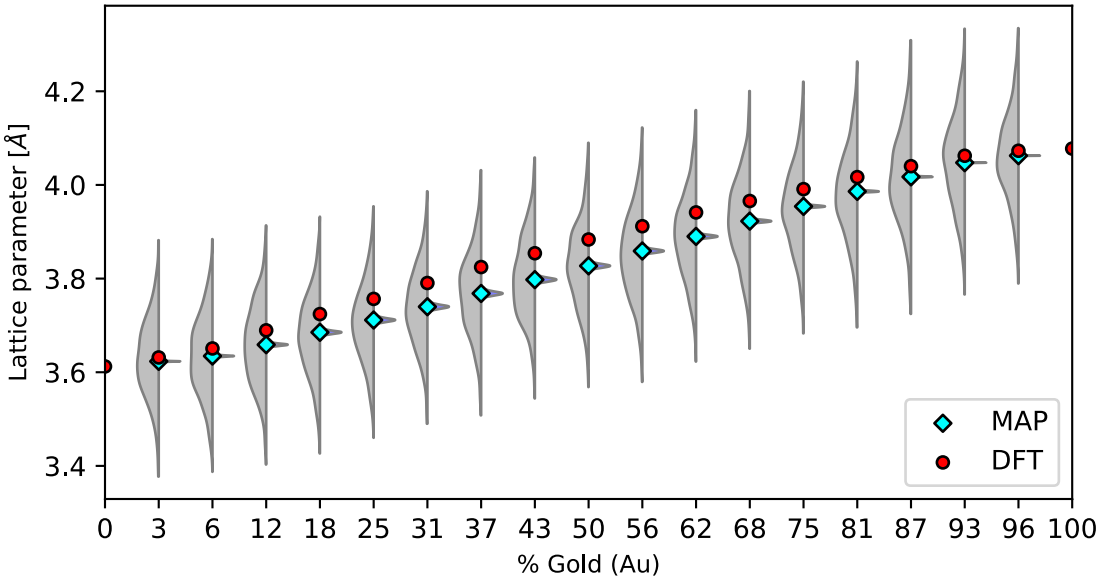

Results: QoI predictions

posterior predictive (left, grey), pushforward posterior (right, blue)

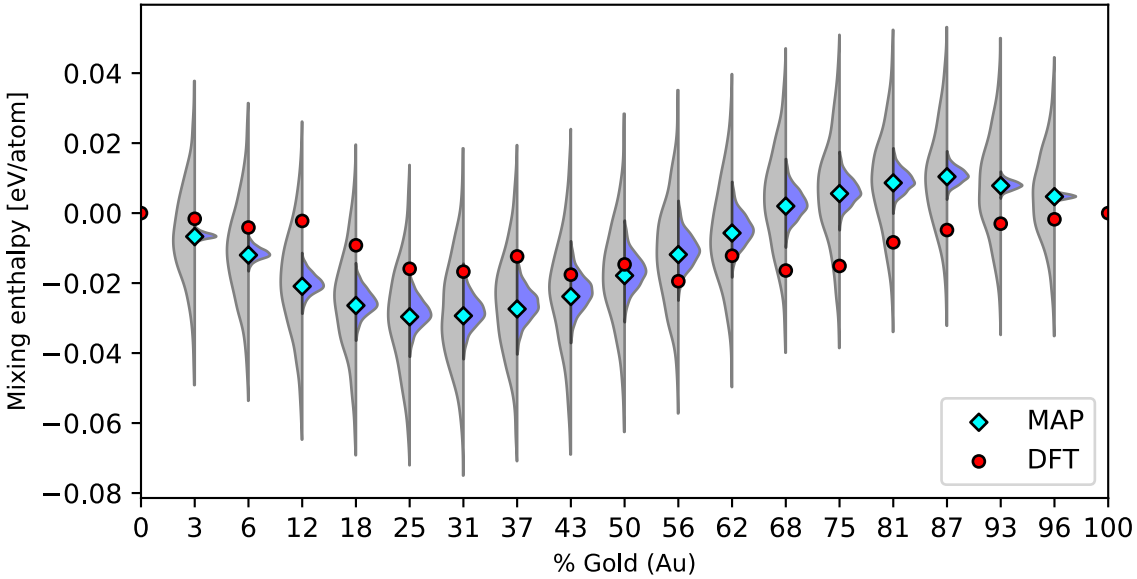

Results: QoI predictions

posterior predictive (left, grey), pushforward posterior (right, blue)

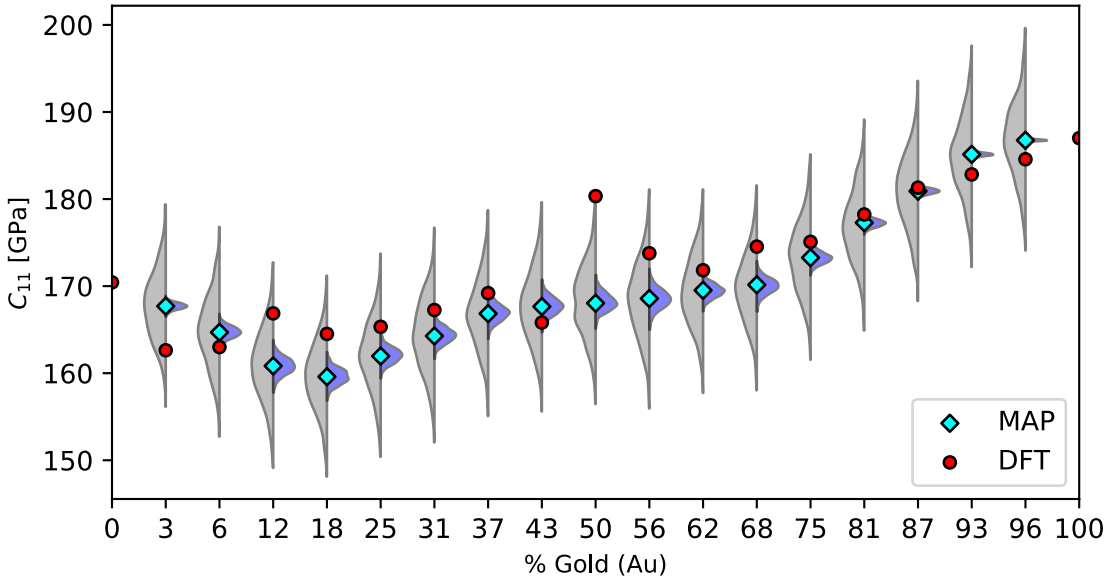

Results: QoI predictions

posterior predictive (left, grey), pushforward posterior (right, blue)

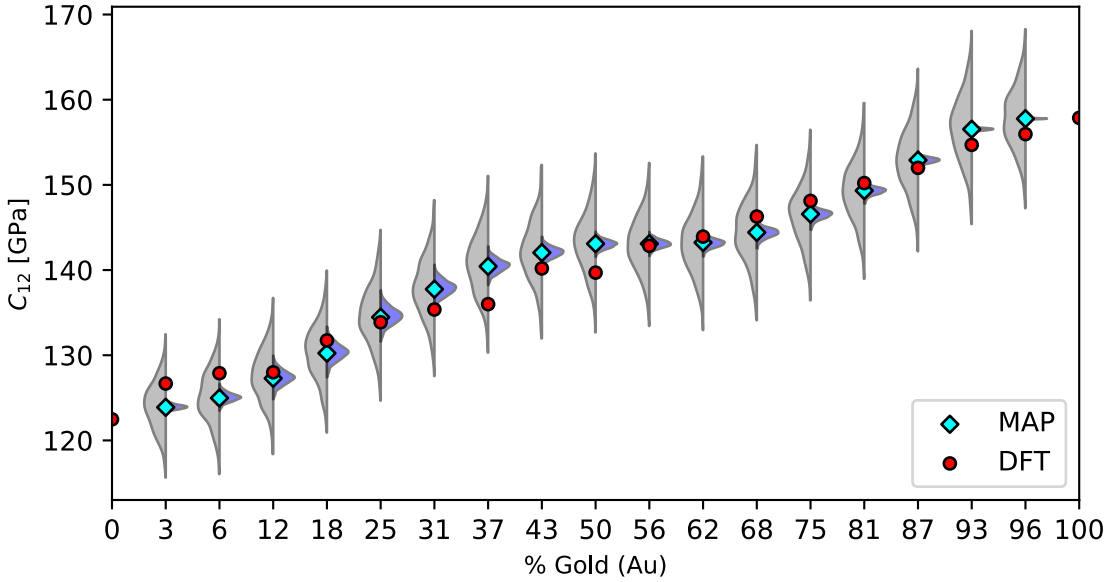

Results: QoI predictions

posterior predictive (left, grey), pushforward posterior (right, blue)

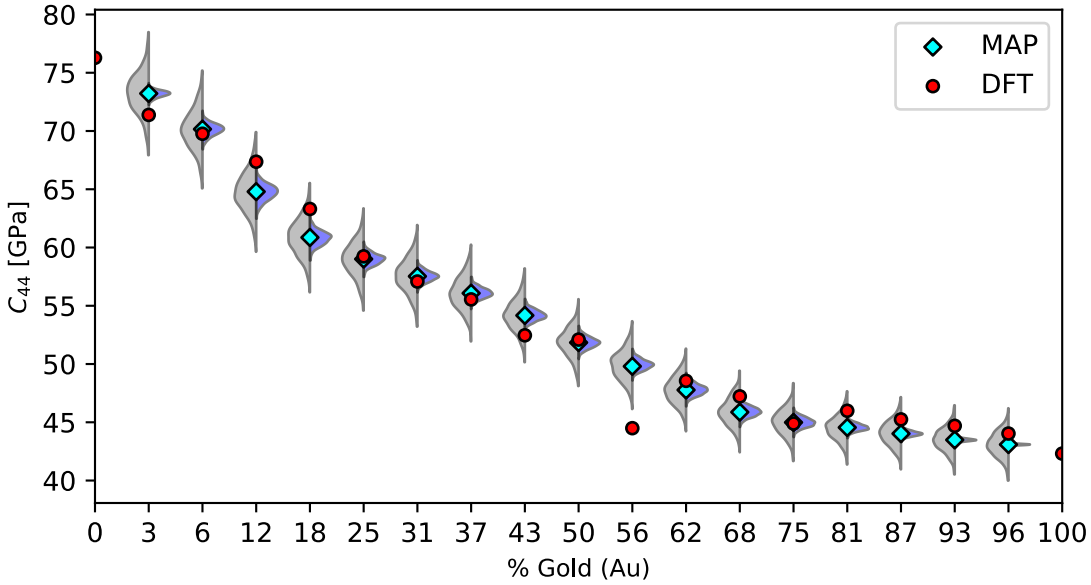

Results: QoI predictions

posterior predictive (left, grey), pushforward posterior (right, blue)

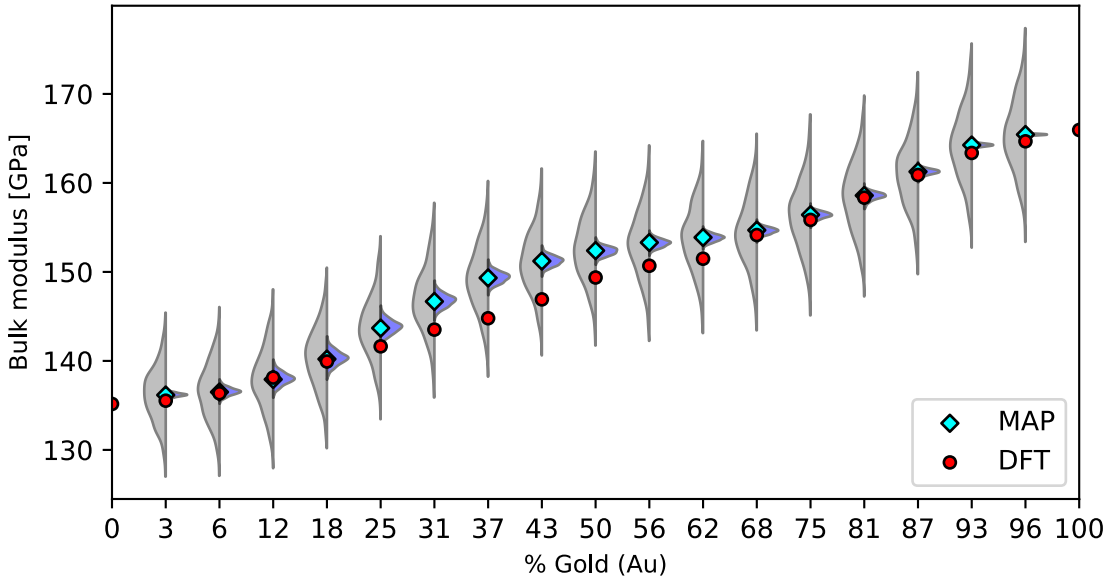

Calibration discussion

- PPDs
  - input: full posterior of model parameters & hyperparameters
  - in general, predictive uncertainty covers DFT data
- PFPs
  - input: marginal posterior of model parameters
  - in general, predictive uncertainty does **not** cover the DFT data

the **level of predictive uncertainty** communicated by just the uncertainty in the model parameters **$p(\theta|y)$** does **not** reflect the actual discrepancy between model predictions and data.

Calibration discussion

- PPDs
  - input: full posterior of model parameters & hyperparameters
  - in general, predictive uncertainty covers DFT data
- PFPs
  - input: marginal posterior of model parameters
  - in general, predictive uncertainty does **not** cover the DFT data

the **level of predictive uncertainty** communicated by just the uncertainty in the model parameters **$p(\theta|y)$** does **not** reflect the actual discrepancy between model predictions and data.

Challenge for prediction

Examining force predictions

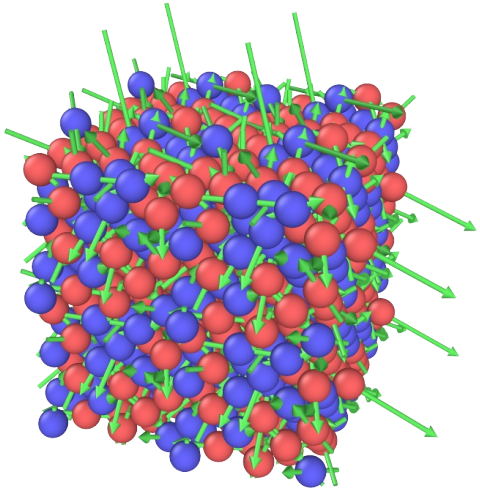

Forces are a QoI not included in the calibration, and hence may be used to assess the calibrated potential through comparison with DFT.

Predictions are of the PFP-type and based on the marginal posterior $p(\theta|y)$:

- no sensible mechanism for transferring our additive model error from the calibration QoIs to force predictions
- UQ perspective: previous calibration results suggest that the predictive uncertainties will be underestimated and overconfident

Force prediction are lacking

parity plots for pure elements (benchmarks)

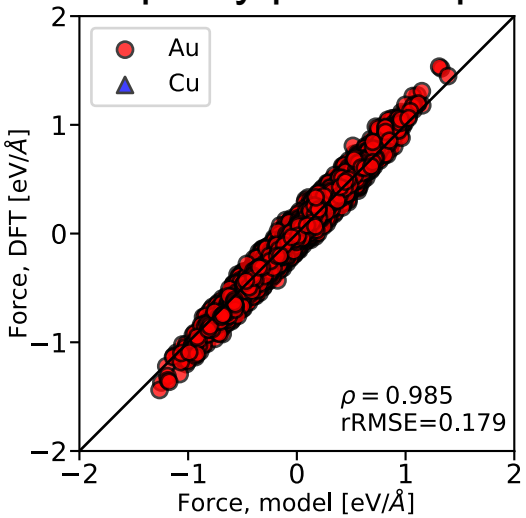

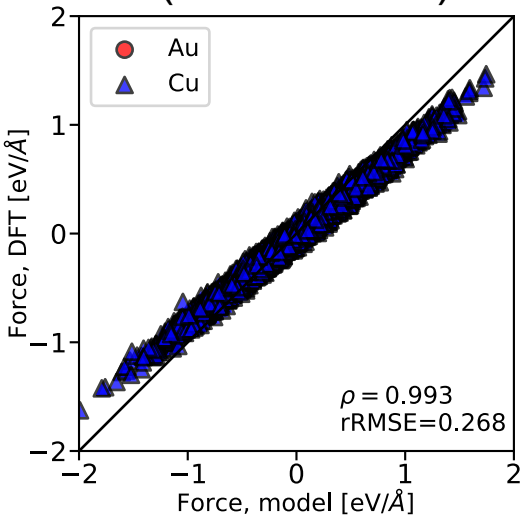

parity plot for 50%-50% composition (MAP parameter only)

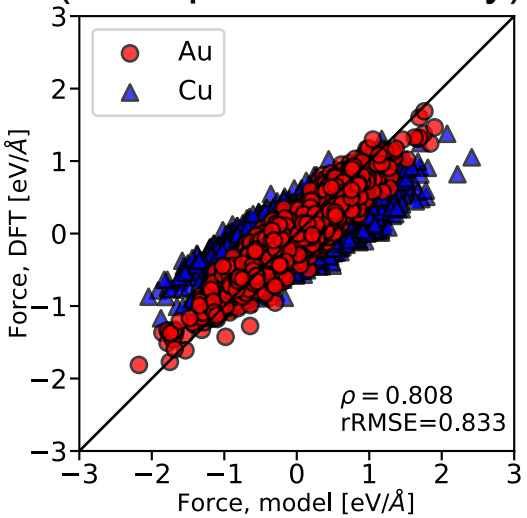

error metrics: correlation coefficient, normalized RMSE.

Pushforward posterior distributions of one error metric:

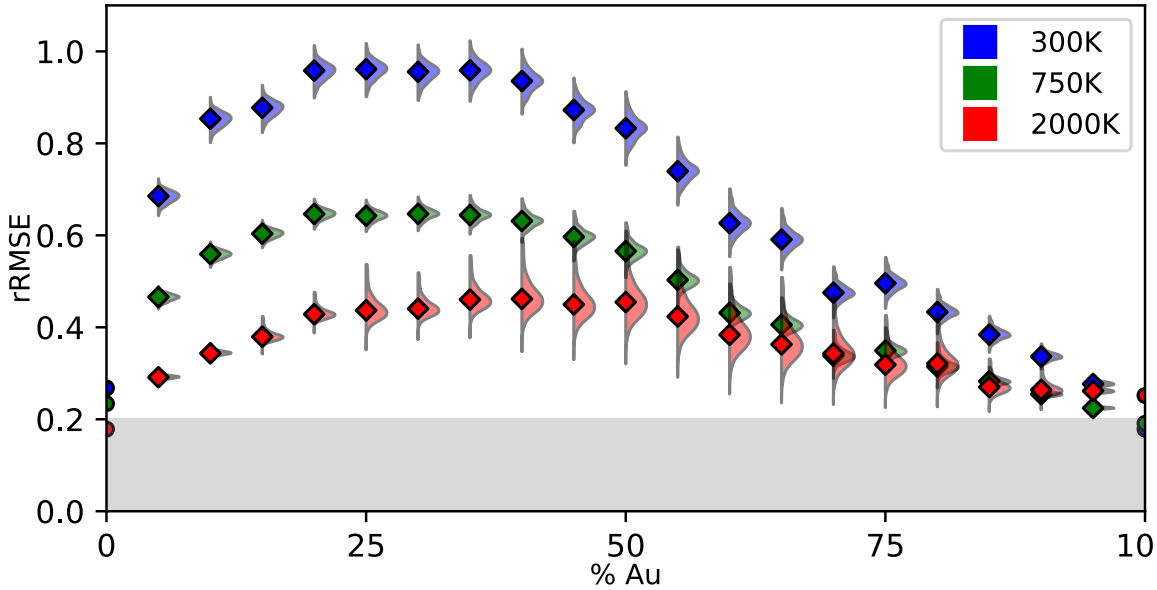

for comparison, relative error range for the calibration QoIs.

The calibrated potential model is not predictive of forces.
These results motivate the **inclusion of force data** in the calibration QoIs.

Summary

- Investigated RAMPAGE potential model for Au-Cu systems
- Implemented a sequential strategy for Bayesian calibration
  - iterative inference steps with locally constructed gaussian processes
  - guided by an expensive physical model
- Highlighted the role of model error in calibration and prediction
  - e.g., differences between PFPs and PPDs.
  - results motivate the inclusion of embedded forms of model error that can be more readily transferred to other prediction settings (such as forces).
- Predictive assessments exposed key limitations of the model
  - inadequate force predictions motivate inclusion of force data in training.

Acknowledgements

AH, **CS**, and **HN** are supported by the U.S. Department of Energy, Office of Science:

- Advanced Scientific Computing Research (ASCR)
- Scientific Discovery through Advanced Computing (SciDAC) program through the FASTMath Institute
- National Energy Research Scientific Computing Center (NERSC)

EW and **WW** are supported by:

- Air Force Office of Scientific Research (AFOSR) under Contract No.FA9550-19-1-0378
- Ohio Supercomputer Center, Project No. PAS0072

Sandia National Laboratories is a multi-mission laboratory managed and operated by National Technology and Engineering Solutions of Sandia, LLC., a wholly owned subsidiary of Honeywell International, Inc., for the U.S. Department of Energy's National Nuclear Security Administration under contract DE-NA-0003525. The views expressed in the presentation do not necessarily represent the views of the U.S. Department of Energy or the United States Government.

Extra slides

Simulation workflow

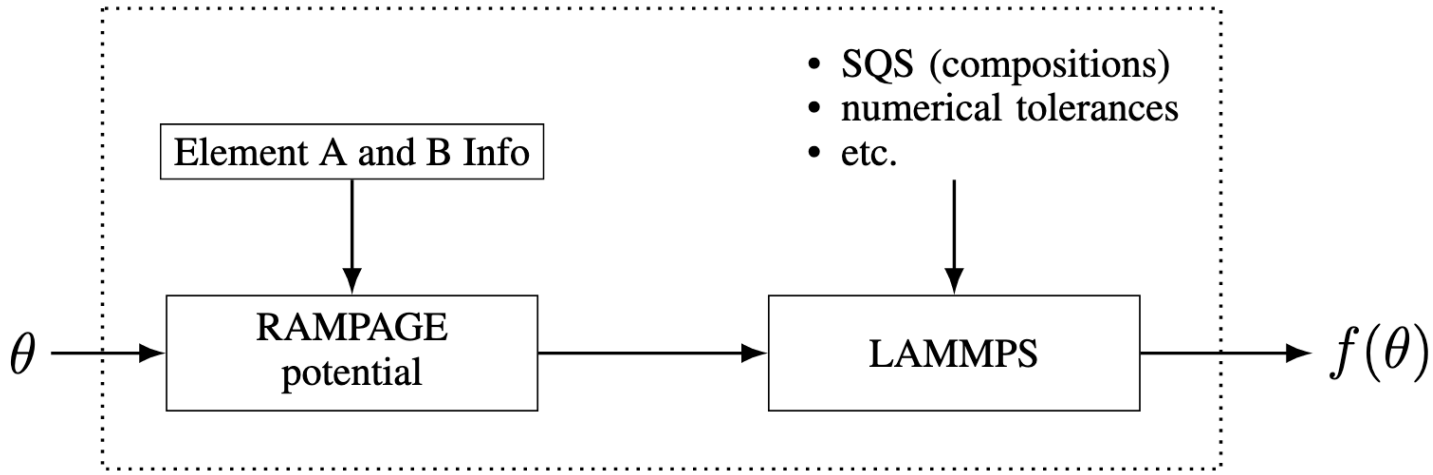

Figure 1: Simulation workflow for a generic binary system. Here, θ represents the input parameter vector for the examined IAP, and $f(\theta)$ the vector of output QoI values.

Inference strategy

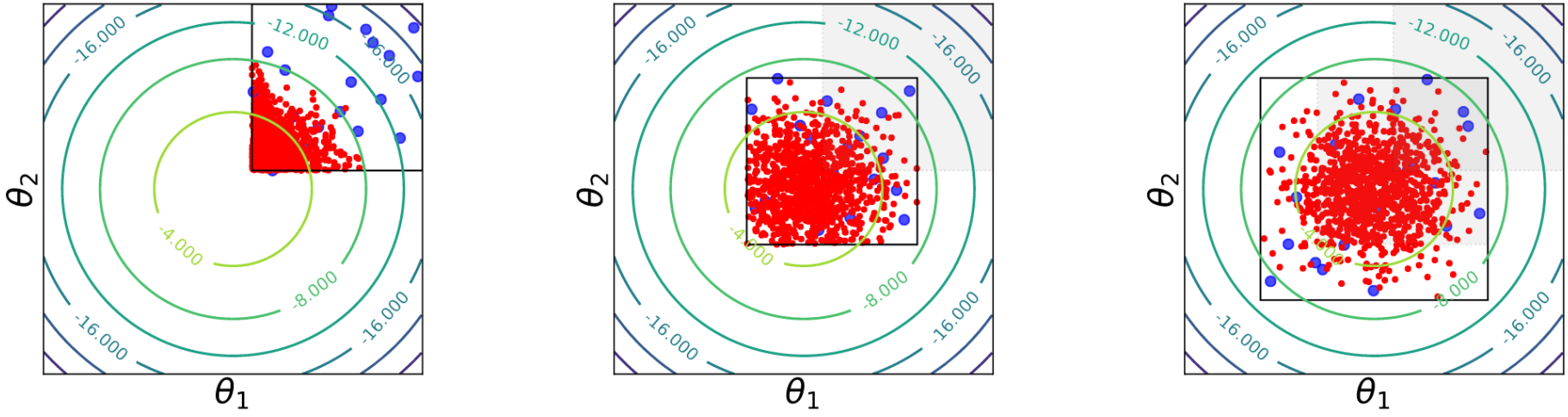

Figure 3: Toy example illustrating the movement of $\mathcal{H}$ during the inference strategy.

Forces workflow

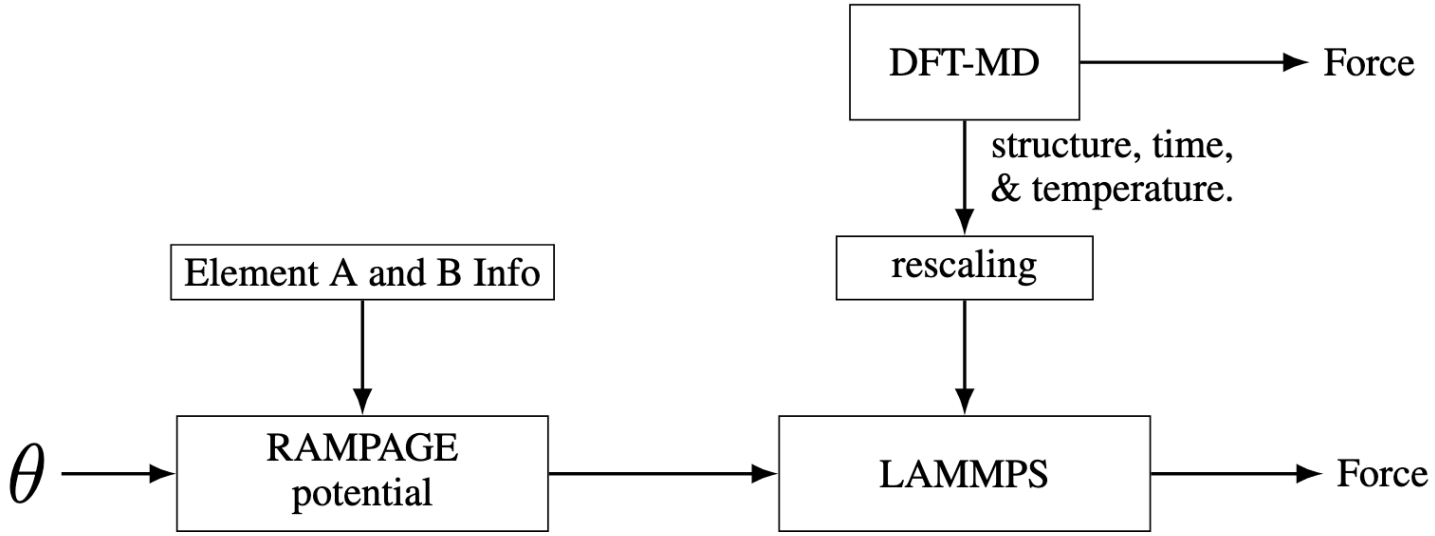

Figure 12: Molecular dynamics simulation workflow for computing forces.

Force error metrics

$$\rho = \frac{\sum_{j\in\mathcal{J}} \left(F_j^{\text{model}} - \overline{F}^{\text{model}}\right)\left(F_j^{\text{DFT}} - \overline{F}^{\text{DFT}}\right)}{\sqrt{\sum_{j\in\mathcal{J}} \left(F_j^{\text{model}} - \overline{F}^{\text{model}}\right)^2}\sqrt{\sum_{j\in\mathcal{J}} \left(F_j^{\text{DFT}} - \overline{F}^{\text{DFT}}\right)^2}}$$

$$\text{RMSE} = \sqrt{\frac{1}{|\mathcal{J}|}\sum_{j\in\mathcal{J}} \left(F_j^{\text{model}} - F_j^{\text{DFT}}\right)^2} \tag{16}$$

$$\text{rRMSE} = \frac{\text{RMSE}}{\sqrt{\frac{1}{|\mathcal{J}|}\sum_{j\in\mathcal{J}} \left(F_j^{\text{DFT}}\right)^2}},$$

where all summations are taken over time steps, atoms, and components, and

$$\overline{F} = \frac{1}{|\mathcal{J}|}\sum_{j\in\mathcal{J}} F_j \tag{17}$$

$$\mathcal{J} = \{(t, a, c) : t \in \text{time},\ a \in \text{atoms},\ c \in \{x, y, z\}\}.$$

PFPs for correlation coefficients (forces)

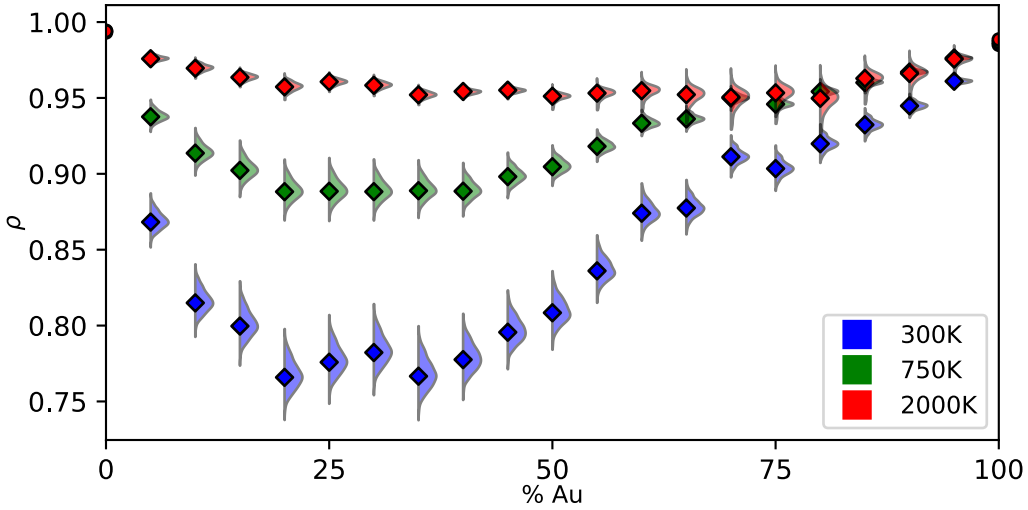

Surrogate modeling error

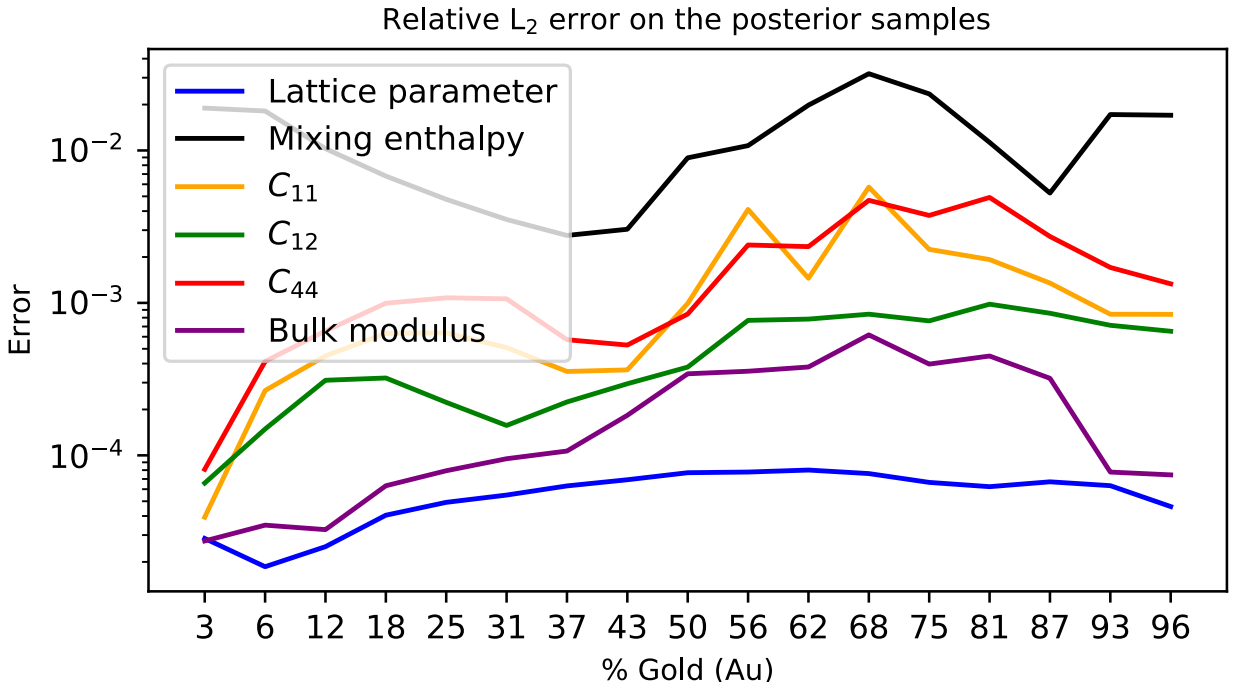

$$\frac{\sqrt{\sum_{i=1}^{m}\left(y_{\mathrm{SURR}}(\theta_i)-y_{\mathrm{LAMMPS}}(\theta_i)\right)^2}}{\sqrt{\sum_{i=1}^{m} y_{\mathrm{LAMMPS}}(\theta_i)^2}}$$

Surrogate modeling error

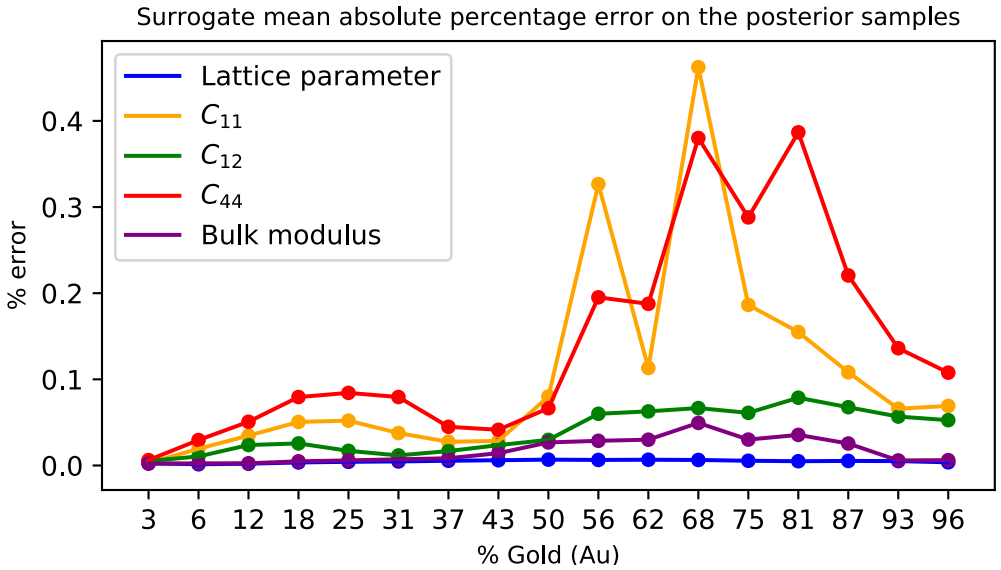

To be removed

Thursday, April 14
MS90
Quantifying Predictive Uncertainty with Physics-Informed Machine Learning - Part II of III
8:10 AM - 10:10 AM
Room: Augusta F - 7th Floor
For Part I, see MS31
For Part III, see MS134
Uncertainty quantification plays a central role in verifying and validating computational models and enabling predictive science. Due to the high computational cost in modeling and simulation, it is desirable to replace the underlying physics model with data-driven surrogate models. However, such data-driven approaches do not capture critical properties and physics. This minisymposium focuses on the research and development of physics-informed, physics-constrained, and physics-guided data-driven surrogate models that also enable uncertainty quantification. We cordially invite researchers to submit work that involves or is related to computationally efficient, reliable, accurate, physics-informed, physics-constrained, physics-guided, and data- and domain-informed surrogate models and methods with an emphasis on uncertainty quantification